

A simple technique for the determination of mechanical strain in thin films with applications to polysilicon

H. Guckel, T. Randazzo,^{a)} and D. W. Burns

Department of Electrical & Computer Engineering, University of Wisconsin, Madison, Wisconsin 53706

(Received 3 August 1984; accepted for publication 15 November 1984)

Free standing, doubly supported micromechanical beams which are fabricated from films with built-in compressive strain fields buckle at critical geometries. Experimental determination of the onset of buckling for known geometries leads to a direct measurement of the strain level in the films. This idea is supported by appropriate theory for experimental structures which form clamped, doubly supported beams with constant cross section and varying lengths. Application to low pressure chemical vapor deposition polysilicon leads to the conclusion that strain fields of 0.2% reduce to 0.05% during annealing.

INTRODUCTION

Semiconductor technologies employ substrates which are decorated with a variety of thin films. Differences in thermal expansion coefficients between the substrate and the deposited films are a primary source for mechanical strain fields. Thus, a substrate-film combination which is annealed to zero strain at some process temperature would be expected to have a strain level which is proportional to the product of the thermal expansion coefficient difference and the process to ambient temperature change. Modifications in this predictable strain value occur and point to other sources for built-in strain fields. Nucleation conditions and high deposition rates which are typical in CVD films can produce highly strained films. Subsequent oxidations modify the built-in strain further.

Electronic device performance degrades when high strain fields are present. Increases in leakage currents are typical and lead to severe problems in dynamic MOS circuits which increase with size reductions. Increased etch and diffusion rates in strained regions are common and reduce yield. High compressive strains are undesired for mechanical structures where they cause wrinkling in thin diaphragms and buckling in beams.

The importance of strain fields and their somewhat uncertain origin make accurate strain measurements a necessity. The goal, precise and easily implemented techniques for local rather than average strain field determination, is difficult to achieve. X-ray techniques are available but do require specialized equipment. Radius of curvature measurements with real rather than optically flat substrates have been used to determine the average rather than local strain field.¹ Elongation measurements of clamped beam overhangs are acceptable but require destructive measurement techniques.² They are also troublesome when large elongations are involved which can lead to plastic deformations or beam buckling. However, buckling itself offers an alternative for the accurate determination of compressive strain fields in thin films. This was first noticed in work at Wisconsin which involves the fabrication of doubly supported polysilicon

beams. Beams with identical cross sections but changing lengths were found to be perfectly straight and free of bowing below a critical length and buckled above this cutoff point. A sharp, strain related threshold appeared evident and held the promise for an accurate, simple measurement of compressive strains. An understanding of the relationship between buckling load, beam geometry and material parameters had to be developed together with a process for the construction of beams with known boundary conditions and geometries for optical microscope determination of the unknown strain field.

Buckling loads for beams

IC technology lends itself to the production of rectangular beams with constant thickness h and cross section A . The moment of inertia I for beams of this type is $(1/12)Ah^2$. Each cross section of the beam supports an axial load P which is assumed to be constant and uniformly distributed. This load and an externally applied transverse load $q(x)$, in force per unit length, combine to deflect the beam by the beam position dependent distance w . The deflection will depend on the density ρ and Young's modulus E of the uniform, isotropic beam material. The differential equation for beam deflection is given by^{3,4}

$$EI \frac{\partial^4 w}{\partial x^4} + P \frac{\partial^2 w}{\partial x^2} + \rho A \frac{\partial^2 w}{\partial t^2} = -q(x). \quad (1)$$

Beams do have resonances. Self-resonances are computed by removing all external forcing functions. The transverse load $q(x)$ is therefore 0 for this type of computation. P , the axial load, remains nonzero because it is due to the built-in strain. Increases in P evidently will cause decreases in the self-resonance. Sufficiently large axial strains will produce a situation for which the smallest resonant frequency becomes 0. This condition causes buckling and is associated with a specific value of P which must be determined. This is readily accomplished by using separation of variables, i.e., $w(x,t)$ is assumed to be of the form $X(x)T(t)$, and by letting $q(x)$ in Eq. (1) go to 0. The result is

$$\frac{1}{T} \frac{d^2 T}{dt^2} = -\frac{EI}{\rho A} \frac{1}{X} \frac{d^4 X}{dx^4} - \frac{P}{\rho A} \frac{1}{X} \frac{d^2 X}{dx^2} = -\omega^2, \quad (2)$$

where ω is the beam frequency. The solutions to Eq. (2) are

^{a)} Present address: Sperry Corporation, Semiconductor Operations, Eagan, Minnesota 55122.

given by

$$T(t) = C_1 \cos(\omega t + \theta), \quad (3)$$

and

$$X(x) = C_2 \sinh \frac{ax}{L} + C_3 \cosh \frac{ax}{L} + C_4 \sin \frac{bx}{L} + C_5 \cos \frac{bx}{L}, \quad (4)$$

where C_1, C_2, C_3, C_4, C_5 , and θ are unknown constants and

$$a^2 = -\frac{PL^2}{2EI} + \left[\left(\frac{PL^2}{2EI} \right)^2 + \omega^2 \frac{\rho AL^4}{EI} \right]^{1/2}, \quad (5)$$

and

$$b^2 = a^2 + PL^2/EI. \quad (6)$$

L is the length of the beam which is supported at $x = 0$ and $x = L$. The nature of the support is introduced through the boundary conditions. Thus

$$X(0) = X(L) = \frac{d^2X}{dx^2} \Big|_{x=0} = \frac{d^2X}{dx^2} \Big|_{x=L} = 0 \quad (7)$$

and

$$X(0) = X(L) = \frac{dX}{dx} \Big|_{x=0} = \frac{dX}{dx} \Big|_{x=L} = 0 \quad (8)$$

identify simple and clamped boundary conditions, respectively. They are readily visualized by sketching the anticipated beam deflections. Both cases are observed in physical structures and therefore deserve attention.

When Eq. (7) or (8) is used in Eq. (4) a 4×4 determinant results which must vanish for nonzero integration constants. This can only be satisfied if a and b and, therefore, ω take special values, i.e., the system is resonant. The detailed computations are somewhat tedious but not very difficult. For simply supported beams the results are

$$b = n\pi, \quad \omega^2 = \frac{(n\pi)^2 EI}{\rho AL^4} \left((n\pi)^2 - \frac{PL^2}{EI} \right) \quad (7a)$$

where $n = 1, 2, 3, \dots$

The buckling load is therefore given by

$$P = \pi^2 EI / L^2. \quad (7b)$$

The associated strain is

$$\epsilon_s = \frac{P}{AE} = \frac{\pi^2 h^2}{12L^2}. \quad (7c)$$

Clamped boundary conditions are more complicated. The determinant equation for this case is given by

$$(a^2 + b^2) \sinh a \sin b - 2ab(1 - \cosh a \cos b) = 0. \quad (8a)$$

The resonant frequencies are solutions of this transcendental equation. An explicit expression for ω which would correspond to the result given in Eq. (7a) is not possible. However, the limit case $\omega \rightarrow 0$ can be studied and yields $b = 2\pi$. The buckling strain is therefore given by

$$\epsilon_c = \frac{P}{AE} = \frac{\pi^2 h^2}{3L^2}. \quad (8b)$$

Equations (7c) and (8b) contain the needed data for strain analysis. Buckling for rectangular beams which are simply supported or clamped is only a function of beam geo-

metry and not material parameters. This is obviously a highly desirable property for the use of beam buckling as a strain measurement tool.

Beam fabrication

Beams for strain field diagnostics are composed of a free standing portion and two symmetrical supports. It is normally possible and advantageous to fabricate the supports from the same material as the beam by simply making the attached portion of the structure very much larger than the free standing part. The end result is a flat, dumbbell-like structure for which clamped boundary conditions can be obtained and can be verified optically.

Two specific processes have been used to fabricate test beams. In the first process substrates such as silicon, sapphire and silicon dioxide are coated with a spacing material. Silicon dioxide, silicon nitride, polysilicon, polyimide, photoresist, and a host of metals form suitable spacers. The material under investigation is deposited on the spacer and defined with a single photomask. An etching procedure is then used to remove the spacer locally, i.e., the supports are undercut by a small fraction of their total area. The etch is designed so that only the spacer is removed. A second technique employs a (100) silicon substrate. It is furnished with an etch resistant layer for hydrazine or potassium hydroxide etching. The beam material is again deposited on this layer and patterned. The silicon substrate under the beam is removed by etching from the backside. A second etch is used to dissolve the etch stop. The end result of either process are beams of constant thickness. Widths and lengths are determined by the single, necessary photomask. Experimental results yield the conclusion that clamped boundary conditions are the rule. Buckling, as described by Eq. (8), is established by fabricating beams of similar topology but changing lengths and by observing beam deformation with an interference contrast microscope. Figure (1) demonstrates the beam

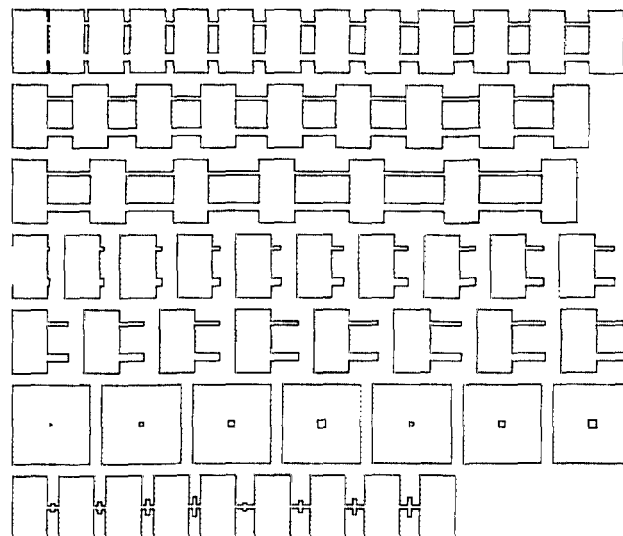


FIG. 1. The strain diagnostic mask defines two beam widths of 10 and 20 μm . Doubly supported beams vary in length from 5 to 160 μm . Cantilevers extend up to 90 μm from their supports.

mask which contains double supported structures as well as cantilevers. The choice of lengths is dictated by the expected strain level for the given thickness. The length increment ΔL fixes the accuracy of the measurement. Thus

$$\frac{\Delta\epsilon_c}{\epsilon_c} = -2\frac{\Delta L}{L}, \quad (8c)$$

which follows from Eq. (8b), predicts increasing accuracy for

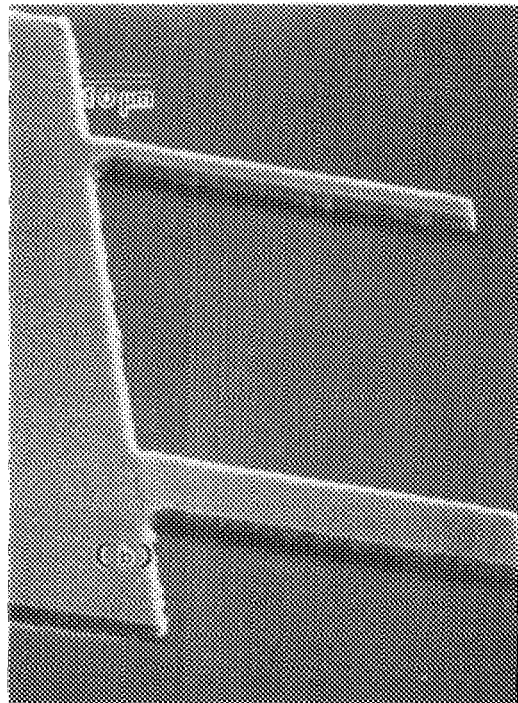
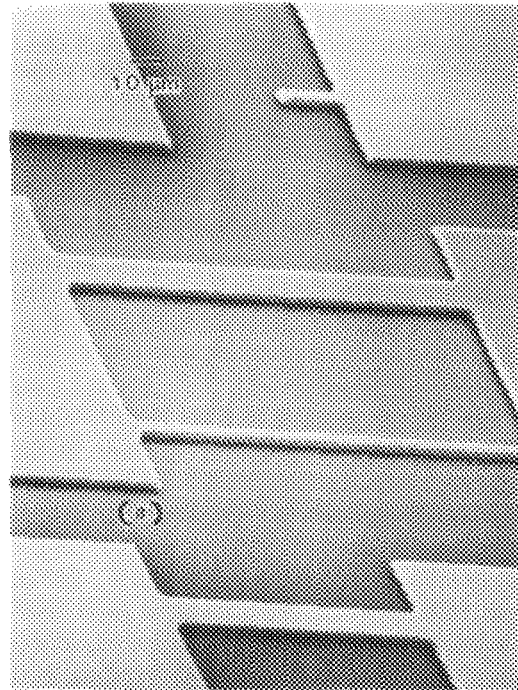


FIG. 2. Patterned polysilicon structures are free standing after the spacer oxide is removed under the beams. 130- μm -long doubly supported beams can be seen in Fig. 2(a), and cantilevers in Fig. 2(b). Cantilevers will show nonuniformities in the strain field with thickness.

long and therefore thicker beams because ΔL becomes a small fraction of the buckling length.

The analysis as given here assures that the strain field is constant over the beam cross section. Buckling strain measurements for various thicknesses which can be obtained by varying the deposition conditions or by thinning existing structures can be used to estimate mild nonuniformities. Severe, unidirectional bowing prior to buckling is associated with strong strain field variations which requires modifications for the buckling criteria.

Application to polysilicon

Polysilicon which is readily deposited by low pressure chemical vapor deposition techniques has possible applications in micromechanics.⁵⁻⁷ The design of pressure transducers and resonant structures requires a priori knowledge of the built-in strain field and its modifications during processing. The behavior of typical polysilicon was studied by using the buckling mode.

Silicon wafers were cleaned and oxidized for 4.5 h at 1150 °C. This produced a silicon dioxide spacer of 1.5 μm . The oxide was covered with LPCVD polysilicon.⁸ The deposition temperature was 650 °C. Pure silane at 300 m Torr for 1.5 h produced an undoped film of 1.56 μm . The wafers were split into two lots. For lot No. 1 anneal cycles of 3 h at various temperatures were used. The wafers were then oxidized at 830 °C for 1 h in a wet ambient. Lot No. 2 was first oxidized and then annealed. The wafers were patterned with the mask of Fig. 1. Buffered HF was used to define the oxide. A 1% HF in HNO₃ mixture formed the silicon etch. The spacer was removed by inserting the wafer in concentrated HF. Water and methanol rinses follow this procedure and yield

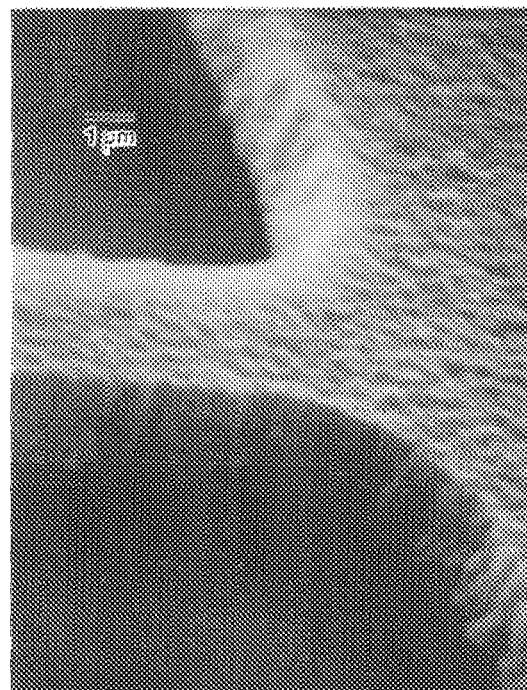


FIG. 3. Clamped boundary conditions are demonstrated for doubly supported beams.

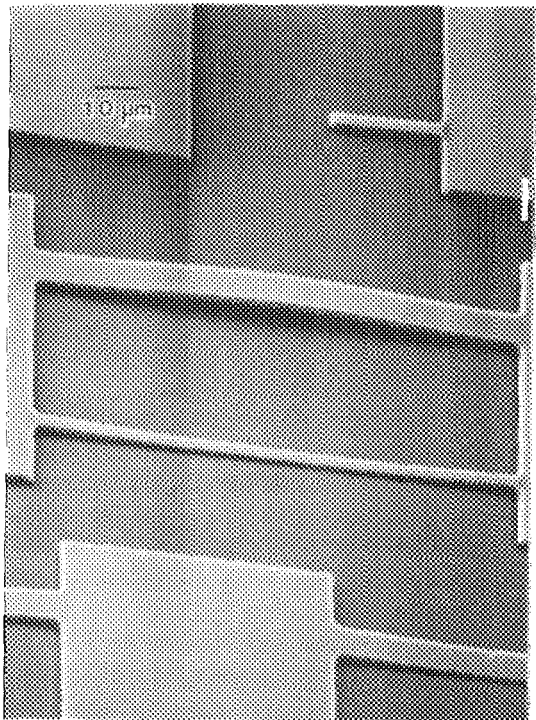


FIG. 4. Doubly supported beams longer than the critical length will buckle in a compressive strain field as shown by these 150- μm beams.

samples for optical inspection. No difficulty with surface tension was experienced.

Figures 2(a) and 2(b) are the results for unbuckled, straight beams. The cantilevers which are easily distorted by liquid etching problems are straight, a fact which is shared with the doubly supported structures. The undercut support is shown in Fig. 3. It is straight and yields the desired clamped boundary condition. Figure 4 shows the buckled configuration which produces up or down displacements of doubly supported structures. Cantilevers typically bend down and are permanently deformed if contact with the sub-

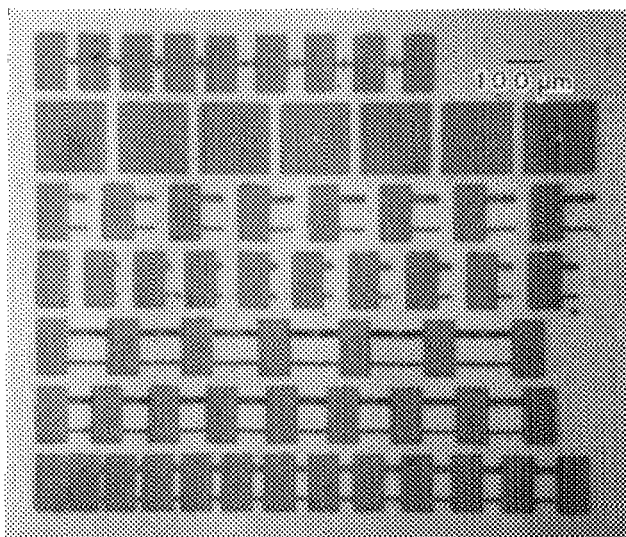


FIG. 5. Buckled beams are readily identified using an interference contrast microscope. Chip area is 1600 by 1300 μm .

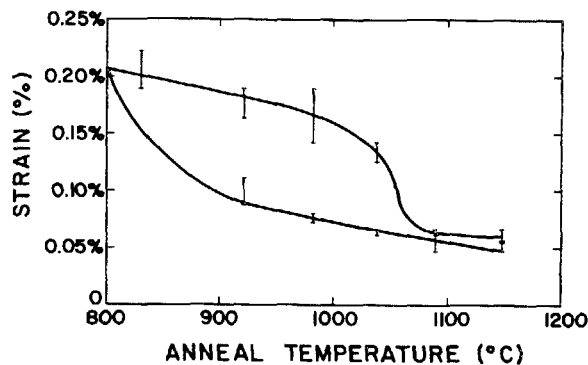


FIG. 6. The strain in a composite film consisting of 1.56 μm of polysilicon and a 700 \AA masking oxide is determined using buckled beam data. Wafers annealed for 3 h in a nitrogen ambient and then oxidized (upper curve) have a higher compressive strain field at moderate anneal temperatures than wafers oxidized before annealing (bottom curve).

strate is established. Figure 5 demonstrates the ease with which buckling can be detected by interference contrast techniques. Data from lot No. 1 and lot No. 2 was collected by this method and converted to strain data. Figure 6 illustrates the effect of the anneal cycles on the strain field. Samples which are annealed together with the masking oxide show a rapid decrease in strain field from slightly above 0.2% to roughly 0.05% at 1100 $^{\circ}\text{C}$. The pressure in the beams varies therefore between 4000 to 1000 atm. Annealing before oxidation always produces an increased strain field in the medium temperature regions. Decreases occur as the softening point of silicon dioxide, i.e., near 970 $^{\circ}\text{C}$, and of course also near 1100 $^{\circ}\text{C}$ where the polysilicon layer itself exhibits strain reductions. Both samples, as expected, anneal to the same strain value at 1100 $^{\circ}\text{C}$. A minimum strain level of 0.05% is achieved for this particular film. Therefore the type of beam which is used here will remain unbuckled only if

$$L < \frac{\pi h}{\sqrt{1.5 \times 10^{-3}}} \quad (9)$$

is satisfied. This is a fundamental limitation on some micro-mechanical structures. Efforts to reduce built-in strain by impurity doping and via composite beams are in progress and will be reported on later.

The test pattern of Fig. 5 utilizes a very small portion of a typical silicon wafer. Measurements of strain variation over wafer surfaces become therefore feasible. Use of this technique has identified the cleaning cycle prior to deposition as one source of strain nonuniformity. Additional rinsing corrected the problem. Variations from deposition to deposition were traced to small changes in reactor leak rate. This was corrected. The end result is wafers with little if any strain variation across the wafer surface. The strain level in these properly controlled films depends on deposition conditions. The detailed behavior has not been studied. However, ramping via an initial low growth rate was examined. It produces polysilicon films with high strain levels and, of course, results in strain fields which vary with thickness.

¹H. Guckel, R. Brown, R. Niemann, and R. Pieper, "Interferometric Measurement of Surface Oxide and Doping Stresses in Silicon Wafers," Report

ECE-80-4, Department of Electrical Engineering, University of Wisconsin, Madison, February 1980.

²P. G. Borden, *Appl. Phys. Lett.* **36**, 829 (1980).

³S. Timoshenko and J. Gere, *Mechanics of Materials* (Van Nostrand Reinhold, New York, 1972).

⁴D. J. Gorman, *Free Vibration Analysis of Beams and Shafts* (Wiley, New

York, 1975).

⁵R. T. Howe and R. S. Muller, *J. Electrochem. Soc.* **130**, 1420 (1983).

⁶R. T. Howe and R. S. Muller, *Sensors and Actuators* **4**, 447 (1983).

⁷R. T. Howe and R. S. Muller, *J. Appl. Phys.* **54**, 4674 (1983).

⁸T. I. Kamins, M. M. Mandurah and K. C. Saraswat, *J. Electrochem. Soc.* **125**, 927 (1978).